Imaging the coexistence of a superconducting phase and a charge-density modulation in the $K_{0.73}Fe_{1.67}Se_2$ superconductor using a scanning tunneling microscope

Peng Cai,[1] Cun Ye,[1] Wei Ruan,[1] Xiaodong Zhou,[1] Aifeng Wang,[2] Meng Zhang,[2] Xianhui Chen,[2] and Yayu Wang[1,*]

[1]*State Key Laboratory of Low Dimensional Quantum Physics, Department of Physics, Tsinghua University, Haidian, Beijing 100084, People's Republic of China*

[2]*Hefei National Laboratory for Physical Science at Microscale and Department of Physics, University of Science and Technology of China, Hefei, Anhui 230026, People's Republic of China*

(Received 19 January 2012; published 23 March 2012)

We report scanning tunneling microscopy studies of the local structural and electronic properties of the iron selenide superconductor $K_{0.73}Fe_{1.67}Se_2$ with $T_C = 32$ K. On the atomically resolved FeSe surface, we observe a well-defined superconducting gap and the microscopic coexistence of a charge-density modulation with $\sqrt{2} \times \sqrt{2}$ periodicity with respect to the original Se lattice. We propose that a possible origin of the pattern is the electronic superstructure caused by the block-antiferromagnetic ordering of the iron moments. The widely expected iron vacancy ordering is not observed, indicating that it is not a necessary ingredient for superconductivity in the intercalated iron selenides.

DOI: 10.1103/PhysRevB.85.094512 PACS number(s): 74.55.+v, 74.25.Dw, 74.62.Bf, 74.70.Xa

I. INTRODUCTION

The iron-based superconductors have attracted tremendous recent interest due to the promise of solving high T_C superconductivity (SC) via a new route.[1,2] Similar to the cuprates, the iron compounds also possess a complex phase diagram involving a variety of structural, electronic, and magnetic phases.[3] A key task in finding the mechanism of SC is to clarify the nature of each phase and its implications to SC. For example, the existence of antiferromagnetic (AF) ordering in close proximity to SC in the iron pnictides suggests that spin fluctuation may play a crucial role in mediating the Cooper pairing.[4] On the other hand, the discovery of nematic electronic ordering in the parent state of 122 pnictide suggests that stripelike models may be highly relevant.[5]

The intricate interplay between various phases is prominently exemplified in the new iron selenide superconductors $A_xFe_ySe_2$ (A = K, Rb, Cs, Tl, etc.) with T_C above 30 K.[6–11] Due to the distinct Fermi surface (FS) topology from their pnictide counterparts,[12–14] $A_xFe_ySe_2$ are expected to be ideal test grounds for theoretical models of iron-based SC. However, due to the chemical off-stoichiometry and spatial inhomogeneities in $A_xFe_ySe_2$, a consensus regarding the lattice, electronic, and magnetic structures of the SC phase is still lacking. Muon spin rotation (μSR) experiment on $Cs_{0.8}(FeSe_{0.98})_2$ detects the microscopic coexistence of SC and AF[15] and suggests that the two orders are closely related. Neutron scattering on $K_{0.8}Fe_{1.6}Se_2$ reveals the formation of the Fe vacancy ordering and block-checkerboard-AF phase at elevated temperatures,[16,17] which has prompted the proposal of Fe vacancy-ordered Mott insulator as the parent state.[18–20] Transport and magnetization studies suggest that $A_xFe_ySe_2$ is an AF insulator for Fe content $1.5<y<1.6$, and SC emerges only for $y>1.8$ when many of the Fe vacancies are filled.[9,11,21] To make it more complicated, x-ray diffraction (XRD)[22] and transmission electron microscopy (TEM)[23] reveal the separation of $A_xFe_ySe_2$ into multiple phases with varied A and Fe contents.

Scanning tunneling microscopy (STM) represents an ideal probe for resolving these controversies owing to the unique capability of detecting the local structural and electronic properties simultaneously. In this paper we report atomic-scale STM studies of the $K_{0.73}Fe_{1.67}Se_2$ single crystals with $T_C = 32$ K. On the atomically resolved FeSe layer without Fe vacancy, we observe an unexpected $\sqrt{2} \times \sqrt{2}$ charge-density modulation coexisting with the SC phase. Comparison to theoretical calculations shows that the electronic superstructure is caused by the block-AF ordering in the Fe layer, which implies a microscopic coexistence of SC and AF. No sign of iron vacancy is observed on this surface, indicating that it is not necessary for SC to occur in the intercalated iron selenides.

II. EXPERIMENTAL

High-quality $K_{0.73}Fe_{1.67}Se_2$ single crystals are grown by the Bridgeman method.[7] The chemical composition of the crystal is calibrated by using energy-dispersive x-ray spectrometer mounted on field emission scanning electron microscope (Sirion200). For STM experiments, polycrystalline tungsten tips are prepared and calibrated on the Au(111) surface as described elsewhere.[24] $K_{0.73}Fe_{1.67}Se_2$ single crystals are cleaved *in situ* at 77 K and then immediately transferred into the STM stage, which stays at 5 K in ultrahigh vacuum better than 5×10^{-11} mbar. All the data shown here are obtained at the base temperature $T = 5$ K. The STM topography is taken in the constant current mode, and the dI/dV spectroscopy is collected by standard ac lock-in method with a modulation frequency $f = 423$ Hz.

III. RESULTS AND DISCUSSION

The resistivity and Meissner effect have been measured on the $K_{0.73}Fe_{1.67}Se_2$ crystals studied here. Fig. 1(a) shows the sharp SC transition at $T_C = 32$ K, and Fig. 1(b) reveals two consecutive phase transitions at much higher T. The increase of resistivity at $T_S = 546$ K is usually ascribed to the $\sqrt{5} \times \sqrt{5}$ Fe vacancy ordering, and the drop of susceptibility at $T_N = 535$ K indicates the appearance of AF ordering.

Figure 2(a) shows the schematic 122-type crystal structure of KFe_2Se_2, which consists of FeSe layers of edge-shared $FeSe_4$ tetrahedra separated by the intercalated K atoms. The

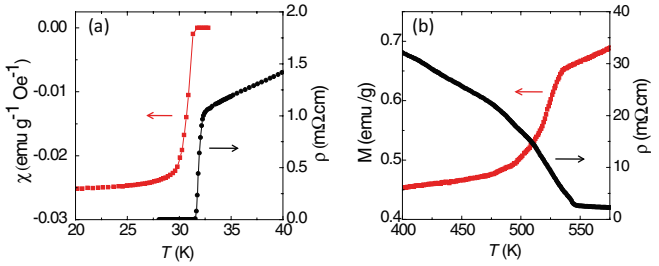

FIG. 1. (Color online) (a) The Meissner effect ($H_\perp = 10$ Oe) and resistivity curves show a sharp SC transition at $T_C = 32$ K. (b) The increase of resistivity at $T_S = 546$ K is due to the iron vacancy ordering and the drop of magnetization ($H_{//} = 50$ kOe) at $T_N = 535$ K indicates the AF ordering.

crystal is expected to cleave between two adjacent FeSe layers, exposing the Se-terminated surface decorated with the remnant K atoms (on average half of the K atoms are left on the surface). Figure 2(b) displays a topographic image of cleaved $K_{0.73}Fe_{1.67}Se_2$ taken with a sample bias $V_s = 0.4$ V and tunneling current $I_t = 5$ pA. The surface shows a rather complex morphology consistent with our expectation. On top of the large flat terrace, there are bright spots either as isolated spheres or small clusters and patches. Figure 2(c) presents a line profile along the red (gray) broken line in Fig. 2(b) and shows that the height of the bright spots is ~1 Å, consistent with the size of K atom. Figure 2(d) displays the derivative plot of the topography of an area with rather sparse K atoms [marked by the dotted green (medium gray) square in Fig. 2(b)], which uncovers an atomically clear square lattice. The lattice constant is around $a = 4$ Å, in agreement with the distance between two adjacent Se atoms of the FeSe layer.

We note that the chance of seeing the atomically resolved surface shown above is about 10% among more than 100 approaches on 12 different $K_{0.73}Fe_{1.67}Se_2$ crystals each being cleaved once. On the rest of the surfaces, we cannot obtain high-quality STM images at $T = 5$ K. A possible explanation is that the majority phase of the sample is insulating so that high-resolution STM imaging is difficult at low T. The

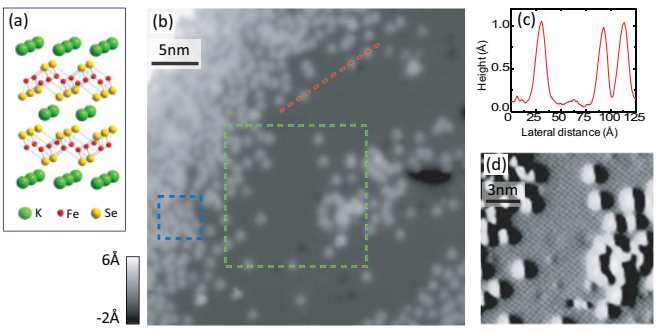

FIG. 2. (Color online) (a) The schematic crystal structure of KFe_2Se_2. (b) STM topography (256 × 256 pixels) of cleaved $K_{0.73}Fe_{1.67}Se_2$ obtained at sample bias $V_s = 0.4$ V and tunneling current $I_t = 5$ pA with scanning speed 1 s/line. (c) Line profile along the red (diagonal) broken line in (b) shows that the height of the bright spots is ~1 Å, consistent with the size of K atoms. (d) Derivative plot of the topography of the area marked in (b) uncovers an atomically clear square lattice with lattice constant $a \sim 4$ Å.

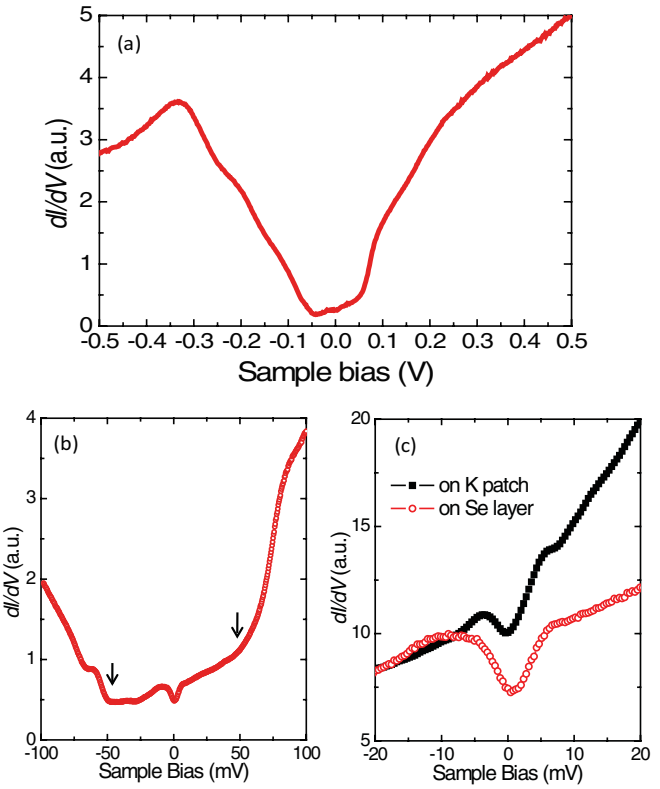

FIG. 3. (Color online) (a) Spatially averaged dI/dV spectrum measured on the flat FeSe surface without K atoms. (b) The low-energy spectrum shows a gaplike feature at ±50 mV (indicated by arrows). (c) The well-defined SC gap with amplitude 2Δ~14 meV exists both on the flat Se surface [red (gray)] and that covered by K atoms (black).

atomically resolved FeSe surface reported here may represent the minority phase of the sample. This is consistent with the recent finding of a phase separation into $\sqrt{5} \times \sqrt{5}$ Fe vacanc-ordered insulating phase and vacancy-free SC phase on (110)-oriented $K_xFe_ySe_2$ film grown by molecular beam epitaxy (MBE).[25]

Figure 3(a) shows the spatially averaged dI/dV curve taken directly on flat Se surface without K atoms. The $dI/dV(V_s, \boldsymbol{r})$ is approximately proportional to the local electron density of state (DOS) of the sample at location $\boldsymbol{r}$ with energy $\varepsilon = eV_s$ (the Fermi level E_F lies at $V_s = 0$). On the negative bias side of Fig. 3(a), which corresponds to the occupied states, the DOS shows a rapid increase starting from about $V_s = -50$ mV and reaches a peak near $V_s = -330$ mV. Very similar features have been seen by angle-resolved photoemission spectroscopy (ARPES) on $A_xFe_ySe_2$ and are ascribed to the appearance of holelike bands below E_F.[26] The positive bias spectrum corresponds to the unoccupied states that cannot be reached by ARPES. The dI/dV curve also shows a similar increase of DOS from V_s~50 to 300 mV, although the features are not as sharp as that in the negative side. The overall dI/dV profile, therefore, represents a broad gaplike DOS suppression between $\varepsilon = \pm 50$ meV around the E_F.

Figure 3(b) displays the low-bias dI/dV curve with higher energy resolution. The most pronounced feature here is a small gap located at E_F with amplitude 2Δ~14 meV. There are

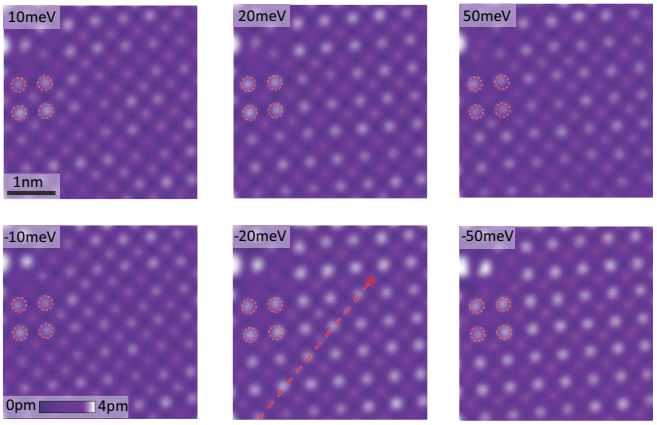

FIG. 4. (Color online) High-resolution images (256 × 256 pixels) on the FeSe surface taken with different sample biases ($V_s = \pm 10$ mV, ± 2mV, ± 50 mV, $I_t = 5$ pA) reveal a bias-dependent $\sqrt{2} \times \sqrt{2}$ superstructure (all the color scales are the same). These images are taken on a small flat area different from that shown in the large overview in Fig. 2.

three different pieces of evidence suggesting that this gap is the SC gap. First, all of our samples have been checked by transport and magnetization to be SC. This gap is the only gap that we have ever observed, and it is always present in all samples. Second, the gap amplitude is in rough agreement with the SC gap observed by ARPES on similar $K_xFe_ySe_2$ crystals with $T_C = 32$ K.[12] The ratio of $2\Delta/k_BT_C$ is around 5, which is beyond the BCS weak coupling limit but in the same range as the 122 iron pnictides.[27] Third, on the area covered with K patches [marked by broken blue (medium gray) lines in Fig. 2(b)], we observe the same gap with rather sharp coherent peaks [Fig. 3(c)], suggesting that it is a robust feature insensitive to the surface morphology. A closer examination shows that the gap is incomplete with finite DOS at E_F that is too large to be explained by thermal activation at $T = 5$ K. This broad and shallow gap structure is seen in all the flat and clean surfaces and thus is an intrinsic property of the system. The exact origin of this behavior is unclear at the moment. One possible explanation is the formation of a polar surface due to the charge imbalance created by cleaving the 122-type surface of $K_xFe_2Se_2$. The electronic structure on the polar surface could be quite different from that of the bulk, which may give rise to much weakened SC. Another fine structure revealed by Fig. 3(b) is the two successive DOS jumps at $\varepsilon = -50$ meV and -66 meV, which was also observed by ARPES.[26] The remarkable agreement between our STM results and the ARPES spectrum suggests that we probe the intrinsic electronic properties of the system.

Figure 4 displays high-resolution close-up images on a small K-free FeSe surface, which reveals a highly unexpected feature. The bright spots marked by circles indicate the existence of a new charge-density modulation pattern. The superstructure has a $\sqrt{2} \times \sqrt{2}$ unit cell with respect to the Se-Se square lattice. In general the feature is quite weak, and the maximum apparent height difference between the bright and dark lattice sites is merely 0.02 Å [Fig. 5(b)]. We argue that this superstructure is electronic in origin rather than from a surface reconstruction because the feature is strongly bias dependent. The superstructures are most pronounced at $V_s = -20$ mV and -50 mV and become weaker at other biases. The patterns cannot be clearly resolved for sample biases higher than ± 100 mV [Fig. 5(a)]. As shown in Fig. 5(c), the superconducting spectrum can be observed in any location of the superstructure, indicating the homogeneous coexistence of SC with the charge-density modulation.

From the STM images alone, we cannot exclude the possibility that the new electronic superstructure is a peculiar surface effect. Recently, the same superstructure has been found by XRD and TEM in similar $K_xFe_ySe_2$ crystals.[22,28] In both experiments, the $\sqrt{5} \times \sqrt{5}$ Fe vacancy ordering is observed at high T, but a weak $\sqrt{2} \times \sqrt{2}$ superstructure emerges at low T. The agreement between the bulk structural studies and our STM images suggests that the $\sqrt{2} \times \sqrt{2}$ superstructure is an intrinsic bulk property.

The coexistence of electronic ordering and SC is a rather common phenomenon in low-dimensional superconductors, including the cuprates, layered chalcogenides, and organic compounds. The mechanism of the electronic ordering and its implications to SC, however, could be a very challenging problem. There usually exists two totally different scenarios: one involves the FS nesting of itinerant electrons, and the other

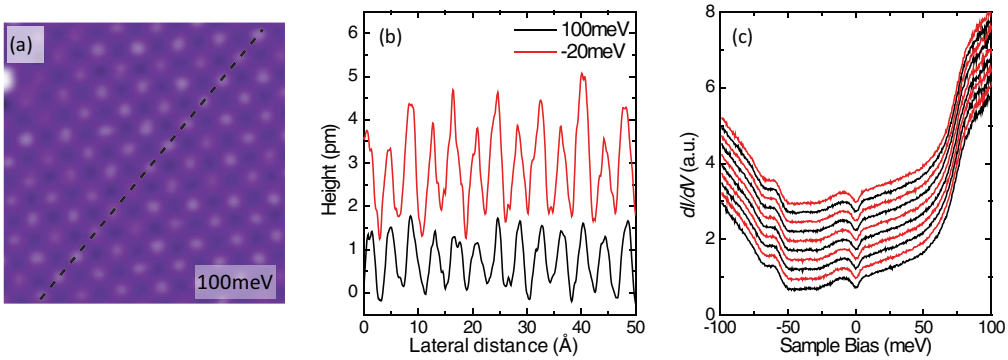

FIG. 5. (Color online) (a) Image taken at higher bias $V_s = 100$ mV (the same area of Fig. 3 with the same color scale) shows no discernable superstructure. (b) The line profile along the black broken line marked in (a) and the red (gray) broken line in Fig. 3 demonstrates the bias dependence of the superstructure (the red curve is offset by 1.5 pm for clarity). (c) Spectra on dark Se [red (gray)] and bright Se (black) sites along the red broken arrow in Fig. 3 are nearly identical.

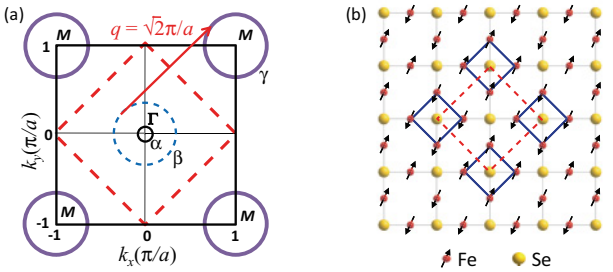

FIG. 6. (Color online) (a) Schematic ARPES-measured FS (black) shows three electronlike FS sheets, two around Γ and one around M. The red arrow along the (π, π) direction indicates the possible nesting vector between the β and γ FS pockets. The red broken line shows the reconstructed BZ by the $\sqrt{2} \times \sqrt{2}$ superstructure. (b) Schematic structure of the top Se surface and the underneath Fe layer with the block-AF structure. The four Fe lattices form a ferromagnetic block (blue solid squares) and a checkerboard pattern. The Se lattices form a $\sqrt{2} \times \sqrt{2}$ superstructure (red broken square) because the nearest neighbor (NN) Se sites become inequivalent.

involves local ordering of certain degree of freedom. A notable example is the checkerboard electronic ordering found in the cuprates.[29,30] While ARPES suggests that the superstructure is due to the charge-density wave (CDW) formed by FS nesting at the antinodal region,[31] comparison with neutron scattering data suggests that it is the charge-density modulation induced by the spin-density wave order.[32] Next we discuss the relevance of these two pictures to the$\sqrt{2} \times \sqrt{2}$ superstructure observed here in $K_{0.73}Fe_{1.67}Se_2$.

The ARPES measured band structure of $K_xFe_ySe_2$ provides some hints for FS nesting[26] in which a weak electronlike FS pocket (the β band) near the Γ point of the Brillouin zone (BZ) with similar size and shape to that around the M point [Fig. 6(a)]. Moreover, the nesting vector between Γ and M will lead to a CDW order with a $\sqrt{2} \times \sqrt{2}$ superstructure, making it an attractive proposal. However, the β band is very weak or even nonexistent in ARPES band maps,[12] and local-density approximation (LDA) calculations cannot reproduce such a large electronlike FS pocket near Γ.[13] Both facts suggest that the β pocket may not be the cause of the nesting but instead might be the consequence of folded FS from the M point when the $\sqrt{2} \times \sqrt{2}$ superstructure is formed.

A more likely origin of the superstructure is certain symmetry breaking states, which may cause a charge-density modulation on the Se layer. Recently, first-principles electronic structure calculation and effective magnetic model analysis have been applied to the magnetic structure of the $K_xFe_ySe_2$ system.[33] It is shown that the ground state of the Fe vacancy-free phase has a block-AF phase in which each four Fe sites group together in a tetragonal structure. The block-AF phase strongly couples to the lattice and leads to a checkerboard phase that quadruples the original Fe lattice, as illustrated in Fig. 6(b). Interestingly, the calculated electron density distribution around the Se atoms above the iron layer shows a $\sqrt{2} \times \sqrt{2}$ charge ordering that exactly matches our STM results. The observed coexistence of the $\sqrt{2} \times \sqrt{2}$ charge ordering with the SC gap suggests that the block-AF phase might be related to the SC.

Another important finding of this work is the absence of Fe vacancy in the SC phase of $K_{0.73}Fe_{1.67}Se_2$. Although the Fe layer lies at 2 Å below the surface, the defect on the Fe site is expected to create pronounced electronic states that can be detected by STM. In the $FeSe_{1-x}Te_x$ and LaOFeAs compounds,[34,35] the Fe site defects can be clearly resolved in STM images as bias-dependent dumbbells due to the tetrahedral bonding between Fe and the surface Se/As atoms. However, our high-resolution STM images on atomically flat FeSe surface of $K_{0.73}Fe_{1.67}Se_2$ [Fig. 4] show no sign of Fe vacancy despite extensive search. Recent STM studies on (110)-oriented MBE-grown $K_xFe_ySe_2$ films also find that the SC phase is the stoichiometric $K_xFe_2Se_2$ without Fe vacancy.[25] The two complimentary STM results demonstrate unambiguously that Fe vacancy ordering is not an essential ingredient for SC in $K_xFe_ySe_2$. This observation calls for a re-examination of the basic assumptions regarding the mechanism of SC. Unlike the viewpoint of doping the iron vacancy-ordered AF Mott insulator, our STM results suggest that the SC phase of $A_xFe_ySe_2$ may be simply viewed as perfect FeSe layers intercalated by K atoms. Recall that T_C of the 11-type FeSe SC can be enhanced from 8.5 K[36] to near 37 K by high pressure.[37] We may hypothesize that in $A_xFe_ySe_2$ the A intercalations provide the charge doping and chemical pressure necessary for the stoichiometric FeSe layers to have high T_C.

IV. CONCLUSION

In summary, atomic-scale STM studies on $K_{0.73}Fe_{1.67}Se_2$ single crystals provide new clues regarding the phase diagram of the intercalated iron selenides. The vacancy-free FeSe layer shows the microscopic coexistence of SC and a charge-density modulation, which is proposed to be caused by the block-AF ordering in the Fe layer. The Fe vacancy ordering is not essential for SC but instead may be related to the insulating phase that is spatially separated from SC. The growth and studies of pure phase superconducting and insulating $K_xFe_ySe_2$ crystals will help to further clarify these issues.

ACKNOWLEDGMENTS

We thank Xi Chen, Donglai Feng, Zheng-Yu Weng, Tao Xiang, Guang-Ming Zhang, Xingjiang Zhou, and especially Jiangping Hu for helpful discussions. This work is supported by the National Natural Science Foundation of China and by the Ministry of Science and Technology of China (Grants No. 2009CB929402, No. 2010CB923003, and No. 2011CBA00101).

*Corresponding author: yayuwang@tsinghua.edu.cn

[1] Y. Kamihara, T. Watanabe, M. Hirano, and H. Hosono, J. Am. Chem. Soc. **130**, 3296 (2008).

[2] X. H. Chen, T. Wu, G. Wu, R. H. Liu, H. Chen, and D. F. Fang, Nature **453**, 761 (2008).

[3] K. Ishida, Y. Nakai, and H. Hosono, J. Phys. Soc. Jpn. **78**, 062001 (2009).

[4]C. de la Cruz, Q. Huang, J. W. Lynn, J. Li, W. Ratcliff II, J. L. Zarestky, H. A. Mook, G. F. Chen, J. L. Luo, N. L. Wang, and P. Dai, Nature **453**, 899 (2008).
[5]T. M. Chuang, M. P. Allan, J. H. Lee, Y. Xie, N. Ni, S. L. Bud'ko, G. S. Boebinger, P. C. Canfield, and J. C. Davis, Science **327**, 181 (2010).
[6]J. Guo, S. Jin, G. Wang, S. Wang, K. Zhu, T. Zhou, M. He, and X. Chen, Phys. Rev. B **82**, 180520(R) (2010).
[7]A. F. Wang, J. J. Ying, Y. J. Yan, R. H. Liu, X. G. Luo, Z. Y. Li, X. F. Wang, M. Zhang, G. J. Ye, P. Cheng, Z. J. Xiang, and X. H. Chen, Phys. Rev. B **83**, 060512(R) (2011).
[8]Y. Mizuguchi, H. Takeya, Y. Kawasaki, T. Ozaki, S. Tsuda, T. Yamaguchi, and Y. Takano, Appl. Phys. Lett. **98**, 042511 (2011).
[9]M.-H. Fang, H.-D. Wang, C.-H. Dong, Z.-J. Li, C.-M. Feng, J. Chen, and H. Q. Yuan, Europhys. Lett. **94**, 27009 (2011).
[10]R. H. Liu, X. G. Luo, M. Zhang, A. F. Wang, J. J. Ying, X. F. Wang, Y. J. Yan, Z. J. Xiang, P. Cheng, G. J. Ye, Z. Y. Li, and X. H. Chen, Europhys. Lett. **94**, 27008 (2011).
[11]D. M. Wang, J. B. He, T. L. Xia, and G. F. Chen, Phys. Rev. B **83**, 132502 (2011).
[12]Y. Zhang, L. X. Yang, M. Xu, Z. R. Ye, F. Chen, C. He, H. C. Xu, J. Jiang, B. P. Xie, J. J. Ying, X. F. Wang, X. H. Chen, J. P. Hu, M. Matsunami, S. Kimura, and D. L. Feng, Nat. Mater. **10**, 273 (2011).
[13]T. Qian, X. P. Wang, W. C. Jin, P. Zhang, P. Richard, G. Xu, X. Dai, Z. Fang, J. G. Guo, X. L. Chen, and H. Ding, Phys. Rev. Lett. **106**, 187001 (2011).
[14]D. Mou, S. Liu, X. Jia, J. He, Y. Peng, L. Zhao, L. Yu, G. Liu, S. He, X. Dong, J. Zhang, H. Wang, C. Dong, M. Fang, X. Wang, Q. Peng, Z. Wang, S. Zhang, F. Yang, Z. Xu, C. Chen, and X. J. Zhou, Phys. Rev. Lett. **106**, 107001 (2011).
[15]Z. Shermadini, A. Krzton-Maziopa, M. Bendele, R. Khasanov, H. Luetkens, K. Conder, E. Pomjakushina, S. Weyeneth, V. Pomjakushin, O. Bossen, and A. Amato, Phys. Rev. Lett. **106**, 117602 (2011).
[16]W. Bao, Q. Huang, G. F. Chen, M. A. Green, D. M. Wang, J. B. He, X. Q. Wang, and Y. Qiu, Chin. Phys. Lett. **28**, 086104 (2011).
[17]V. Y. Pomjakushin, D. V. Sheptyakov, E. V. Pomjakushina, A. Krzton-Maziopa, K. Conder, D. Chernyshov, V. Svitlyk, and Z. Shermadini, Phys. Rev. B **83**, 144410 (2011).
[18]C. Cao and J. Dai, Phys. Rev. B **83**, 193104 (2011).
[19]R. Yu, J.-X. Zhu, and Q. Si, Phys. Rev. Lett. **106**, 186401 (2011).
[20]X.-W. Yan, M. Gao, Z.-Y. Lu, and T. Xiang, Phys. Rev. Lett. **106**, 087005 (2011).
[21]Y. J. Yan, M. Zhang, A. F. Wang, J. J. Ying, Z. Y. Li, W. Qin, X. G. Luo, J. Q. Li, J. Hu, and X. H. Chen, Sci. Rep. **2**, 212 (2012).
[22]A. Ricci, N. Poccia, B. Joseph, G. Arrighetti, L. Barba, J. Plaisier, G. Campi, Y. Mizuguchi, H. Takeya, Y. Takano, N. L. Saini, and A. Bianconi, Supercon. Sci. Technol. **24**, 082002 (2011).
[23]Z. Wang, Y. J. Song, H. L. Shi, Z. W. Wang, Z. Chen, H. F. Tian, G. F. Chen, J. G. Guo, H. X. Yang, and J. Q. Li, Phys. Rev. B **83**, 140505(R) (2011).
[24]C. Ye, P. Cai, R. Yu, X. Zhou, W. Ruan, Q. Liu, C. Jin, and Y. Wang, e-print arXiv:1201.0342.
[25]W. Li, H. Ding, P. Deng, K. Chang, C. Song, K. He, L. Wang, X. Ma, J.-P. Hu, X. Chen, and Q.-K. Xue, Nat. Phys. **8**, 126 (2012).
[26]L. Zhao, D. Mou, S. Liu, X. Jia, J. He, Y. Peng, L. Yu, X. Liu, G. Liu, S. He, X. Dong, J. Zhang, J. B. He, D. M. Wang, G. F. Chen, J. G. Guo, X. L. Chen, X. Wang, Q. Peng, Z. Wang, S. Zhang, F. Yang, Z. Xu, C. Chen, and X. J. Zhou, Phys. Rev. B **83**, 140508(R) (2011).
[27]Y. Yin, M. Zech, T. L. Williams, X. F. Wang, G. Wu, X. H. Chen, and J. E. Hoffman, Phys. Rev. Lett. **102**, 097002 (2009).
[28]J. Q. Li, Y. J. Song, H. X. Yang, Z. Wang, H. L. Shi, G. F. Chen, Z. W. Wang, Z. Chen, and H. F. Tian, e-print arXiv:1104.5340.
[29]J. E. Hoffman, K. McElroy, D.-H. Lee, K. M. Lang, H. Eisaki, S. Uchida, and J. C. Davis, Science **297**, 1148 (2002).
[30]T. Hanaguri, C. Lupien, Y. Kohsaka, D. H. Lee, M. Azuma, M. Takano, H. Takagi, and J. C. Davis, Nature **430**, 1001 (2004).
[31]K. M. Shen, F. Ronning, D. H. Lu, F. Baumberger, N. J. C. Ingle, W. S. Lee, W. Meevasana, Y. Kohsaka, M. Azuma, M. Takano, H. Takagi, and Z.-X. Shen, Science **307**, 901 (2005).
[32]S. Sachdev and S.-C. Zhang, Science **295**, 452 (2002).
[33]W. Li, S. Dong, C. Fang, and J. Hu, e-print arXiv:1110.0372.
[34]T. Hanaguri, S. Niitaka, K. Kuroki, and H. Takagi, Science **328**, 474 (2010).
[35]X. Zhou, C. Ye, P. Cai, X. Wang, X. Chen, and Y. Wang, Phys. Rev. Lett. **106**, 087001 (2011).
[36]F.-C. Hsu, J.-Y. Luo, K.-W. Yeh, T.-K. Chen, T.-W. Huang, P. M. Wu, Y.-C. Lee, Y.-L. Huang, Y.-Y. Chu, D.-C. Yan, and M.-K. Wu, Proc. Natl. Acad. Sci. USA **105**, 14262 (2008).
[37]S. Medvedev, T. M. McQueen, I. A. Troyan, T. Palasyuk, M. I. Eremets, R. J. Cava, S. Naghavi, F. Casper, V. Ksenofontov, G. Wortmann, and C. Felser, Nat. Mater. **8**, 630 (2009).